

## Chromium oxide zirconia solid acid catalyst for *n*-pentane isomerization

Nur Hazirah Rozali Annuar<sup>1</sup>, Aishah Abdul Jalil<sup>2,3</sup> and Sugeng Triwahyono<sup>1,4\*</sup>

<sup>1</sup>Department of Chemistry, Faculty of Science, Universiti Teknologi Malaysia, 81310 UTM Johor Bahru, Johor, Malaysia

<sup>2</sup>Department of Chemical Eng., Faculty of Chemical Eng., Universiti Teknologi Malaysia, 81310 UTM Johor Bahru, Johor, Malaysia

<sup>3</sup>Institute Hydrogen Economy, Universiti Teknologi Malaysia, 81310 UTM Johor Bahru, Johor, Malaysia

<sup>4</sup>Ibnu Sina Institute for Fundamental Science Studies, Universiti Teknologi Malaysia, 81310 UTM Johor Bahru, Johor, Malaysia

\*Corresponding Author: sugeng@utm.my (S. Triwahyono)

### Article history :

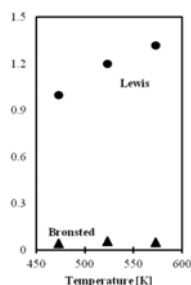
Received 12 December 2013

Revised 10 March 2014

Accepted 1 June 2014

Available online 25 August 2014

### GRAPHICAL ABSTRACT



### ABSTRACT

New catalyst based on zirconia ( $ZrO_2$ ) supported by chromium oxide ( $CrO_3$ ) for isomerization of *n*-pentane was studied.  $CrO_3$ - $ZrO_2$  was prepared with chromium nitrate by the titration and sol-gel technique. The physical properties of the catalysts were characterized by XRD, BET surface area analyzer, and TEM. The acidity and structure of catalysts were determined by pyridine and lutidine preadsorbed FTIR spectroscopy. The isomerization of *n*-pentane was carried out at 523 K under hydrogen stream.  $CrO_3$ - $ZrO_2$  shows the differences in terms of physical properties where the introduction  $CrO_3$  partially eliminated the monoclinic phase of  $ZrO_2$  and developed new peaks assigned to tetragonal phase of  $ZrO_2$ .  $CrO_3$ - $ZrO_2$  also shows a higher specific surface area where it increases in the pore volume of the catalyst compare to its parent zirconia. The IR results indicated that  $CrO_3$ - $ZrO_2$  catalyst have strong Lewis and weak Brønsted acid sites. The conversion of *n*-pentane for  $CrO_3$ - $ZrO_2$  was 32% respectively, while the selectivity to isopentane was 100%.

**Keywords:** Chromium oxide, zirconia, chromium nitrate, ammonium chromate, isomerization of *n*-pentane.

© 2014 Penerbit UTM Press. All rights reserved  
<http://dx.doi.org/10.11113/mjfas.v10n4.321>

## 1. INTRODUCTION

Gasoline is a complex liquid mixture that is processed from petroleum. Among Commonwealth nations, it is known as petrol. It consists of more than 500 hydrocarbons which have five to twelve carbon atoms per molecule. To enhance its performance and reduce emissions, small quantities of alkane cyclic and aromatic compounds, such as toluene and benzene, are added to petrol. It also boosts its octane rating, which is gasoline's measure of resistance. Higher octane levels are needed for high-performance petrol, for example in racing cars, since higher-performance gasoline is more likely to combust.

The operation of a modern refinery nowadays is becoming more and more complex. World-wide public concern about the earth's environment and health considerations led into several new legislative action all around the world. With requirement to meet clean fuels challenge the processing configuration has to be adapted accordingly. Focusing on petrol-fuel, several trends could be identified. In 2003, Germany introduced an ultra-low sulphur gasoline. California has already banned MTBE (methyl tertbutyl eter) from petrol-fuel from few years ago. Therefore oil refiners have to find ways to manage the theoretical octane reduction in the petrol fuel pool. Moreover, managing the toxic benzene content in the petrol-fuel pool in addition to the MTBE problem has also become an important issue [1].

Several major refinery processes to improve Research Octane Number (RON) are isomerization of naphtha, reforming, addition of FCC-Naphtha, alkylation, addition of oxygenates or polygas or butanes. The implications with regard to the new specifications are different for each process [2]. Because of the fact that MTBE and oxygenates contents have to be reduced to a very low level, the most favorable options are alkylation and isomerization due to the straight forward nature of the process and low capital investment.

In this regard, isomerization of light straight alkanes perfectly fits these new trends in processing so called reformulated petrol-fuel. In this context, light straight alkanes isomerization is of particular interest as it can be established in a refinery at low investment, using idle reactors from either catalytic reforming or hydroprocessing. Several research groups have attempted to develop new catalyst for improving the RON of fuel. Robust zeolite based catalyst and chloride alumina based catalyst systems are still the major commercial catalysts, though they have several disadvantages such as low tolerance of contaminant (e.g. sulphur and moisture), high temperature reaction and rapid deactivation of catalysts [3]. Utilization of metal oxides such as  $WO_3$  [4],  $MoO_3$  [5] and strong acids such as sulphuric acid [6], nitric acid and heteropoly acid have been explored to improve the activity, selectivity and stability of catalyst.

In cracking, high molecular weight fractions and catalysts are heated to the point where the carbon-carbon bonds break. Products of the reaction include alkenes and alkanes of lower molecular weight than were present in the original fraction. The alkanes from the cracking reaction are added to the straight-run gasoline to increase the gasoline yield from the crude oil.

On the other hand, development of new type of stable catalyst is required due to reduce the cost of industry. Catalysts used in state-of-the-art isomerization-cracking reactors are bifunctional. Since it has been observed that isomerization of alkanes is the best way in production of liquid fuels or petrol of high quality, solid based acid catalyst plays an important role on providing surface sites for adsorption and conversion of saturated alkanes to branched-chain alkanes. In this study, we prepared CrO<sub>3</sub> loaded zirconia (CrO<sub>3</sub>-ZrO<sub>2</sub>) for *n*-pentane isomerization. The outstanding properties of metal and super acidic material brought a new type of catalyst which is able to overcome the disadvantages of current catalysts.

## 2. EXPERIMENTAL

CrO<sub>3</sub>-ZrO<sub>2</sub> catalyst was prepared by incipient wetness impregnation technique. The precursor used was chromium nitrate nonahydrate (Cr(NO<sub>3</sub>)<sub>3</sub>·9H<sub>2</sub>O) and zirconia, Zr(OH)<sub>4</sub> as support. The support was pretreated with incipient volumes of distilled water. The pretreated support and incipient volumes of solutions containing predetermined amounts of precursor were intimately mixed in order to prepare the catalyst. The resulting material was dried overnight at 383 K followed by calcination at 873 K for 3 hours.

X-Ray Diffraction (XRD) Analysis was used to measure the crystallinity of sample with Bruker Advance D8 X-ray powder diffractometer with Cu Kα (λ = 1.5418 Å) radiation as the diffracted monochromatic beam at 40kV and 40 mA. The data were collected at room temperature over the range of 2θ = 2 - 90° with a scan rate of 0.025° continuously.

Approximately 0.05g of catalyst sample was put into a sample tube holder, and follow by evacuation at 573K for 3h in Quanta Chrome Autosorb-1 spectrometer to measure the surface area of the catalysts. The adsorption of nitrogen then was carried out at 77K.

About 0.07 g sample was ground and pressed in hydraulic press (5000 psi) in order to obtain 13 mm diameter of self supporting wafer before placed in the purpose-made stainless steel IR cell with CaF<sub>2</sub> windows. The cell is connected to a vacuum-adsorption apparatus. Prior to the adsorption measurements, the sample in the cell was evacuated at 598 K. For pyridine adsorption, the sample was exposed to 2 Torr of pyridine at 423 K for 30 min, followed by outgassing at 473 K at 1 h. For 2,6-lutidine adsorption, 4 Torr of 2,6-lutidine was adsorbed on activated samples at room temperature for 30 min followed by outgassing at 373 K. In order to observe the strength and distribution of acidic

sites, pyridine and lutidine adsorption was studied on the sample activated at 473, 523 and 573 K.

Isomerization of *n*-pentane was carried out at 523 K under atmospheric pressure in a continuous flow reactor equipped with an online sampling valve for gas chromatographic analysis. A 0.04 g portion of catalyst was charged into a 10 mm i.d. tubular reactor, and then was subjected to H<sub>2</sub> reduction at 673 K for 12 h (H<sub>2</sub> 30 mL/min). After cooling to reaction temperature in stream of H<sub>2</sub>, pentanes were introduced onto the catalyst bed with flow of H<sub>2</sub> is 30 mL/min. Reaction of pentanes were performed at 573 K. The composition of product was analyzed by FID online gas chromatography equipped with VZ7 packed column.

The selectivity to particular product (S<sub>i</sub>) was calculated according to Eq.(1)

$$S_i = \frac{A_i}{\sum A_i - A_{n\text{-pentane}}} \times 100 \quad (1)$$

where A<sub>i</sub> are corrected chromatographic area for particular compound.

## 3. RESULTS & DISCUSSION

### 3.1 Physical properties of the catalyst

Fig. 1 illustrates the XRD patterns of ZrO<sub>2</sub> and CrO<sub>3</sub>-ZrO<sub>2</sub> catalysts. ZrO<sub>2</sub> exhibits three well established polymorphs which are monoclinic, tetragonal and cubic phase of ZrO<sub>2</sub>. The sharp diffraction lines at 2θ = 28.1°, 31.4°, 33.9° and 38.4° are corresponding to the monoclinic phase of ZrO<sub>2</sub> while the peaks at 2θ = 30.2° and 34.5° are corresponding to the tetragonal phase of ZrO<sub>2</sub>. This result also showed that CrO<sub>3</sub>-ZrO<sub>2</sub> has higher tetragonal phase at 30.2° and 34.5° compare to ZrO<sub>2</sub>. The introduction of CrO<sub>3</sub> on ZrO<sub>2</sub> partially eliminated the peaks assigned to the monoclinic phase of ZrO<sub>2</sub> and developed new peaks assigned to tetragonal phase of ZrO<sub>2</sub>. The presence of CrO<sub>3</sub> inhibits the sintering of ZrO<sub>2</sub> crystallites which led to stabilize the tetragonal phase of ZrO<sub>2</sub>. The relative volume of monoclinic and metastable tetragonal ZrO<sub>2</sub> can be determined by using the Toraya equation. The relative volume of monoclinic and metastable tetragonal phase of ZrO<sub>2</sub> (M/T) showed that CrO<sub>3</sub>-ZrO<sub>2</sub> has lower ratio compare to ZrO<sub>2</sub>. This is due to the low intensity of monoclinic phase of CrO<sub>3</sub>-ZrO<sub>2</sub>. Trunschke et al. reported that for low chromium loadings (0.5-2 wt%), monoclinic and tetragonal zirconia coexist. In catalysts with 4 wt% chromium loading, the tetragonal modification of zirconia predominates. The chromium in CrO<sub>x</sub>/ZrO<sub>2</sub> catalyst also stabilizes the metastable tetragonal phase [7].

Physicochemical analysis by N<sub>2</sub> adsorption-desorption isotherm shows that the BET specific surface area of ZrO<sub>2</sub> and CrO<sub>3</sub>-ZrO<sub>2</sub> are 42 and 150 m<sup>2</sup>/g, respectively where the introduction of CrO<sub>3</sub> tend to increase the surface area of the catalyst. The surface area of the

supported chromium oxide sample is always significantly larger than those of pure zirconia, indicating the inhibition of sintering of  $ZrO_2$  in the presence of  $CrO_3$  compound [8,9].

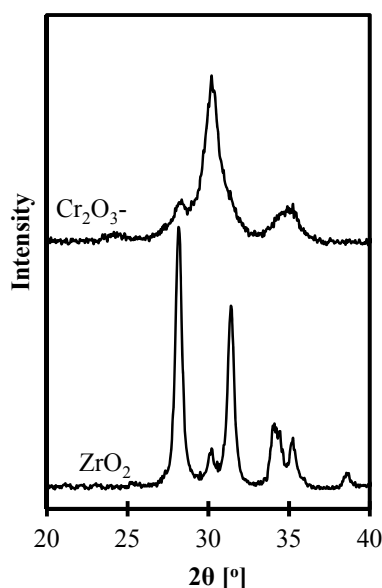


Fig. 1 X-Ray Diffraction patterns of  $ZrO_2$  and  $Cr_2O_3$ - $ZrO_2$ .

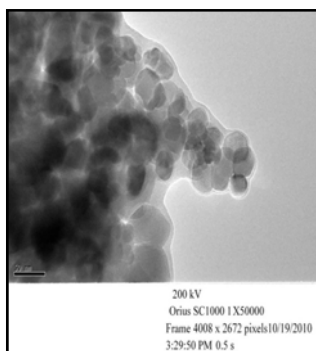


Fig. 2 TEM image of  $Cr_2O_3$ - $ZrO_2$ .

Fig. 2 shows the TEM image of nano  $Cr_2O_3$ - $ZrO_2$  where the catalyst was regularly granular in shape, and the size distribution of this particle was very narrow. Nevertheless, the relatively good agreement between BET surface area and the particle size from TEM image indicated that single crystalline particles of this sample was separable.

### 3.2 Intrinsic acidity of $CrO_3$ - $ZrO_2$ catalyst.

The type of acid sites in  $CrO_3$ - $ZrO_2$  was qualitatively probed by pyridine molecule in which the adsorption was monitored by IR spectroscopy. Fig. 3 (A) shows the acidic sites of  $Cr_2O_3$ - $ZrO_2$  in the region of  $1600$ - $1400\text{ cm}^{-1}$  as a function of pyridine adsorbed on  $CrO_3$ - $ZrO_2$  at different temperatures. For dotted lines, it represents the pyridine-

preadsorbed  $ZrO_2$  catalyst.  $ZrO_2$  sample shows a band at  $1445\text{ cm}^{-1}$  possesses to Lewis acid sites due to the presence of  $\text{cus } Zr^{4+}$  [10]. The modification of  $ZrO_2$  with  $CrO_3$  induced a Brønsted acid sites at  $1545\text{ cm}^{-1}$  and increased the intensity at  $1445\text{ cm}^{-1}$  contributed by pyridine coordinatively bonded to Lewis acid sites. The band centered at  $1480\text{ cm}^{-1}$  can be ascribed to the conjugation of protonic and Lewis acid sites [11]. There is also a water deformation band observed at  $1575\text{ cm}^{-1}$  where it can also be assigned to a hydronium ion,  $H_3O^+$ . As the pretreatment temperature increased, the band at  $1445\text{ cm}^{-1}$  increased, while the band at  $1545\text{ cm}^{-1}$  is slightly decreased. These changes are more clearly seen if the absorbances are plotted against the pretreatment temperature of the sample shown in Fig. 3 (B). As the pretreatment temperature was raised, the amount of Lewis acid sites increased while the amount of protonic acid sites is almost constant. Because the outgassing temperature after pyridine adsorption was  $473\text{ K}$ , the acid sites under consideration are those which retained pyridine against outgassing at a relatively low temperature of  $473\text{ K}$ .

From Fig. 3, both Lewis and protonic acid sites are present on the catalysts pretreated with different treatment followed by outgassing at  $473\text{ K}$ . The ratio of Lewis acid sites to protonic acid sites increased with an increase of the pretreatment temperature. This is commonly observed for other mixed metal oxides such as silica–alumina and zeolites. By pretreatment at a higher temperature, dehydration and/or dehydroxylation proceeds, and acidic OH groups are eliminated which contributing to the Brønsted acid site, hence, leaving the Lewis acid sites. In the case of  $CrO_3$ - $ZrO_2$  too, Brønsted acid sites are the surface of OH groups located at certain configurations of Cr and Zr, and Lewis acid sites are generated by removal of the surface OH groups on the same locations where protonic acid sites are (Figure 5) [12].

The nature of acid sites on  $CrO_3$ - $ZrO_2$  is different compare to other solid acid catalyst such as HZSM-5 where HZSM-5 does not have a significant Lewis acidic group at  $1454\text{ cm}^{-1}$  in its parent zeolite. This means that the coordinative  $Al^{3+}$  cations located in the extra framework Al-oxide cluster act as very weak Lewis electron pair acceptor [13]. As for the other based zirconia catalyst such as  $SO_4^{2-}$ - $ZrO_2$  and  $WO_3$ - $ZrO_2$ , they possess strong Brønsted and Lewis acid sites, in addition to a considerable number of weak Brønsted and Lewis acid sites on  $SO_4^{2-}$ - $ZrO_2$  and only weak Lewis acid sites on  $WO_3$ - $ZrO_2$  [12].

Lutidine (2,6-Dimethylpyridine) is known to be a more probe of Brønsted acid site than pyridine due to its higher basicity and to the steric hindrance of the methyl groups. Fig. 4 shows the IR spectra of lutidine adsorbed on zirconia and chromium oxide zirconia between  $1675$  and  $1520\text{ cm}^{-1}$ . For unmodified  $ZrO_2$  sample, the absorbance bands centered at  $1605$  and  $1580\text{ cm}^{-1}$  is assigned to physisorbed species and a species H-bonded to some surface OH groups. These bands are characteristic of the vibrations of 2,6-dimethylpyridine coordinated to a Lewis acid sites. After the introduction of  $CrO_3$  on  $ZrO_2$ , the Lewis acid sites region shows the band at  $1605$ ,  $1595$  and  $1580\text{ cm}^{-1}$ . The

band at 1595  $\text{cm}^{-1}$  gives a broad and asymmetric peak indicates the presence of tetragonal  $\text{ZrO}_2$  where is ascribed as both physisorbed and H-bonded 2,6-lutidine species [10]. After the adsorption of lutidine at room temperature, the band at 1595  $\text{cm}^{-1}$  tends to shift to a higher wavenumber where band at 1605  $\text{cm}^{-1}$  was observed after  $\text{CrO}_3\text{-ZrO}_2$  was heated at 373 K. For Brønsted acid sites, a doublet appeared at 1650 and 1625  $\text{cm}^{-1}$  after the adsorption of lutidine at room temperature attributed to lutidinium ions [14]. These two medium weak bands confirm that the presence of acidic anions induces the appearance of a relatively modest amount of surface Brønsted acidic sites. The shoulder band at 1645  $\text{cm}^{-1}$  indicates the presence of t- $\text{CrO}_3\text{-ZrO}_2$  on Brønsted acid sites. After the sample was heated at 373 K, band at 1645  $\text{cm}^{-1}$  tend to shift to 1640  $\text{cm}^{-1}$  revealed that that the introduction of  $\text{CrO}_3$  on  $\text{ZrO}_2$  develop weak Brønsted acid sites and strong Lewis acid sites. For both Brønsted and Lewis acid sites, the intensity of the bands tend to decrease after heated at 373 K. As the activation temperature of  $\text{CrO}_3\text{-ZrO}_2$  increased, the progressive increase was noted in the intensity of the bands attributed to the Lewis acid sites and there is slightly decrease for the bands attributed at Brønsted acid sites [15]. This pattern can be related to the changes in pyridine preadsorbed IR spectroscopy.

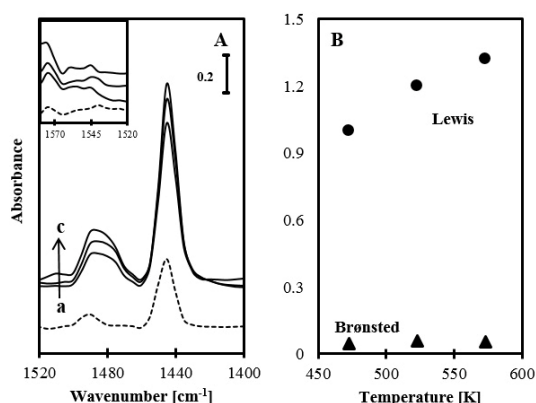


**Fig. 3** A) IR spectra of pyridine-preadsorbed  $\text{Cr}_2\text{O}_3\text{-ZrO}_2$  pretreated at different temperatures. Samples were treated at a) 473 K, b) 523 K, and c) 573 K followed by outgassing at same temperature, 473 K. Pyridine was adsorbed at 423 K. Dotted line represents pyridine-preadsorbed  $\text{ZrO}_2$ . B) Absorbance of IR bands at Brønsted and Lewis acid sites with the temperature of sample treatment for  $\text{Cr}_2\text{O}_3\text{-ZrO}_2$ . (●) Lewis acid site; (▲) Brønsted acid site.

For the other  $\text{ZrO}_2$  based catalyst such as  $\text{WO}_x\text{-ZrO}_2$ , Onfroy et al. reported that the adsorption of lutidine on zirconia give rise to bands at 1610 and 1580  $\text{cm}^{-1}$  characteristic to Lewis acid sites and no Brønsted acid sites were detected. The introduction of  $\text{WO}_x$  on  $\text{ZrO}_2$  arise the bands at 1644 and 1629  $\text{cm}^{-1}$  attributed to Brønsted acid sites. The positions of the peaks were similar for all  $\text{WO}_x\text{-ZrO}_2$  catalyst loading, but their intensity increased with W content. Lower desorption temperature which is 423 K reveals a larger abundance of Brønsted acid sites and a lower threshold for their formation compare to the higher

temperatures which are 523 K and 573 K. The sites detected at 423 K were weakly acidic, as they readily disappear upon heating [14].

### 3.4 Isomerization of n-pentane.

In order to investigate the ability of  $\text{CrO}_3\text{-ZrO}_2$  catalyst towards isomerization of n-alkanes, n-pentane was used as a reactant for the isomerization. This is the preliminary study of catalytic testing in order to make sure the ability of this catalyst towards isomerization. Fig. 5 shows the products distribution of n-pentane isomerization over  $\text{CrO}_3\text{-ZrO}_2$  catalyst at 523 K in a continuous flow reactor. The outlet was composed of iso-pentane and residual n-pentane but no  $\text{C}_1\text{-C}_4$  cracking products and higher hydrocarbon was formed. The selectivity was observed to be 100% and there was no cracking products form during this reaction. The reactivity studies reveal that the activity of  $\text{CrO}_3\text{-ZrO}_2$  depends upon the type of structure of catalyst [16]. The conversion of  $\text{CrO}_3\text{-ZrO}_2$  is 32%. The product distribution of n-pentane isomerization at 120 min time on stream was illustrated in Table 1.

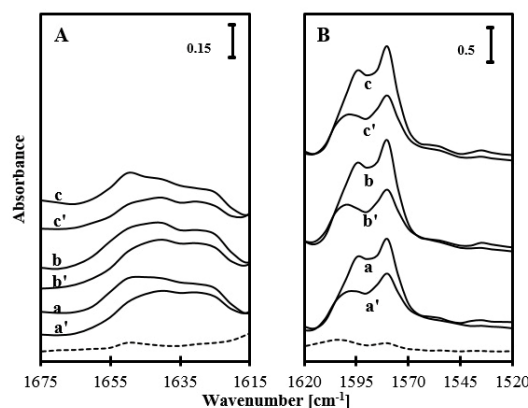


**Fig. 4** IR spectra of lutidine-preadsorbed  $\text{Cr}_2\text{O}_3\text{-ZrO}_2$  pretreated at different temperatures. A) Brønsted acid site and B) Lewis acid site region. Samples were treated at b) 473 K, c) 523 K, and d) 573 K followed by adsorption of lutidine at RT. Primed (') is the samples that were outgassed at 373 K. Dotted line represents lutidine-preadsorbed  $\text{ZrO}_2$  sample.

**Table 1** Product distribution of n-pentane isomerization over  $\text{Cr}_2\text{O}_3\text{-ZrO}_2$  catalyst at 120 min time on stream.

Catalyst	$\text{CrO}_3\text{-ZrO}_2$
Selectivity (%)	100
Conversion (%)	
$\text{C}_1\text{-C}_4$	0
iC <sub>5</sub>	32
$\text{C}_6^+$	0

Sohn et al., reported that the cracking reaction for n-hexane takes place in strong acid sites of  $\text{CrO}_x\text{-ZrO}_2$  while the active site for the dehydrocyclization reaction of n-hexane is  $\text{Cr}^{3+}$  [17]. Kuba et al., studied that the selectivity for isopentane formation remains essentially constant at

about 30% treatment at 523 K, with the products iso-butane, propane, and n-butane and traces of unsaturated hydrocarbons also being observed [18].

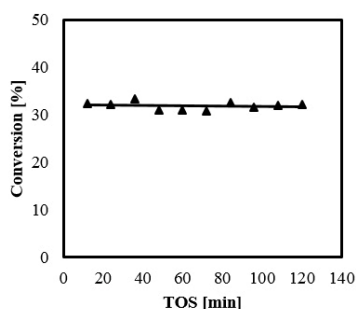


**Fig. 5** Conversion of CrO<sub>3</sub>-ZrO<sub>2</sub> for isomerization of n-pentane at 523 K.

**Table 1** Product distribution of n-pentane isomerization over Cr<sub>2</sub>O<sub>3</sub>-ZrO<sub>2</sub> catalyst at 120 min time on stream.

Catalyst	CrO <sub>3</sub> -ZrO <sub>2</sub>
Selectivity (%)	100
Conversion (%)	
C <sub>1</sub> -C <sub>4</sub>	0
iC <sub>5</sub>	32
C <sub>6</sub> <sup>+</sup>	0

For the isomerization of sulfated zirconia, SO<sub>4</sub><sup>2-</sup>-ZrO<sub>2</sub>, Wakayama et al., observed that high iso-pentane selectivity indicates that the monomolecular reaction is the main route to isomerization and catalyzed by the Lewis acid on SO<sub>4</sub><sup>2-</sup>-ZrO<sub>2</sub>. The production of the small amount of isobutane indicates the small contribution of Brønsted acid sites for the selective isomerization. The Brønsted acid character was not appreciable in pentane isomerization on SO<sub>4</sub><sup>2-</sup>-ZrO<sub>2</sub> because they were not strong enough to form the carbenium ion under the reaction conditions where the catalyst pretreated at 473 K. As for H-beta, the isopentane conversion was much higher than that of pentane and the induction period was extremely short, being less than 30 min. it was treated at 773 K. The high reactivity can be explained by the stability of the tertiary carbenium ion formed on the catalyst surface [19].

#### 4. CONCLUSION

CrO<sub>3</sub>-ZrO<sub>2</sub> was successfully prepared with chromium nitrate by the titration and sol-gel technique.

CrO<sub>3</sub>-ZrO<sub>2</sub> shows the differences in terms of physical properties where the introduction CrO<sub>3</sub> partially eliminated the monoclinic phase of ZrO<sub>2</sub> and developed new peaks assigned to tetragonal phase of ZrO<sub>2</sub>. CrO<sub>3</sub>-ZrO<sub>2</sub> also shows a higher specific surface area where it increases in the pore volume of the catalyst compare to its parent zirconia. The intrinsic acidity of the catalysts was studied by the adsorption of pyridine and lutidine. The IR results indicated that CrO<sub>3</sub>-ZrO<sub>2</sub> catalyst have strong Lewis and weak Brønsted acid sites. The conversion of n-pentane for CrO<sub>3</sub>-ZrO<sub>2</sub> was 32% respectively, while the selectivity to iso-pentane was 100%.

#### ACKNOWLEDGEMENT

This work was supported by Ministry of Science, Technology and Innovation, Malaysia through EScience Fund Research Grant no. 03-01-06-SF0987. Our gratitude also goes to the Hitachi Scholarship Foundation for the Gas Chromatograph Instruments Grant.

#### REFERENCES

- [1] H. Weyda, E. Köhler. *Catal Today*. 81 (2003) 51.
- [2] T. Kimura. *Catal Today*. 81 (2003.) 57.
- [3] M. Khurshid, S.S. Al-Khattaf. *Appl Catal A*. 368 (2009) 57.
- [4] A. H. Karim, S. Triwahyono, A. A. Jalil, H. Hattori. *Appl. Catal. A*. 433-434 (2012) 49.
- [5] S. Triwahyono, A. J. Aishah, S. N. Timmiati, N. N. Ruslan, H. Hattori. *Appl Catal. A*. 372 (2010) 103.
- [6] S. Triwahyono, Z. Abdullah, A. J. Aishah. 2006. *J. Nat. Gas Chem*. 15 (2006) 247.
- [7] A. Trunschke, D. L. Hoang, J. Radnik, H. Lieske. *J. Catal.* 191 (2000) 458.
- [8] M. Scheithauer, R.K. Grasseli, H. Knozinger. *Langmuir*. 14 (1998) 3021.
- [9] E.I. Ross-Medgaarden, W.V. Knowles, T. Kim, M.S. Wong, W. Zhou, C.J. Kiely, I.E. Wachs. *J. Catal.* 256 (2008) 111.
- [10] C. Morterra, G. Meligrana, G. Cerrato, V. Solinas, E. Rombi, M.F. Sini. *Langmuir*. 19 (2003) 5350.
- [11] T. Matsuda, T. Fuse, E. Kikuchi. *J. Catal.* 106 (1987) 38.
- [12] S. Triwahyono, T. Yamada, H. Hattori. *Appl. Catal. A*. 250 (2003) 77.
- [13] J.A. Biscardi, G.D. Meitzner, E. Iglesia, *J. Catal.* 179 (1998) 192.
- [14] T. Onfroy, G. Clet, M. Houalla. *J. Phys. Chem. B*. 109 (2005) 3350.
- [15] V. Lebarbier, G. Clet, M. Houalla. *J. Phys. Chem. B*. 110 (2006) 13909.
- [16] K.L. Furdala, T.D. Tilley. *J. Catal.* 218 (2003) 130.
- [17] J.R. Sohn, S.G. Ryu, H.W. Kim. *J. Mol. Catal.* 135 (1998) 102.
- [18] S. Kuba, P. Lukinskas, R. K. Grasseli, B.C. Gates, H. Knozinger. *J. Catal.* 216 (2003) 356.
- [19] T. Wakayama, H. Matsuhashi, *J. Mol. Catal.* 239 (2005) 36.